Pakistan J. Zool., vol. 56(1), pp 385-393, 2024 DOI: https://dx.doi.org/10.17582/journal.pjz/20220702200702

Mechanism of Antipyretic Effect of Saposhnikoviae Radix Based on Network Pharmacology and Experimental Verification

Taidong Wang[1], Xiaowei Huang[1], Jian Huang[2], Guangfu Lv[3] and Zhe Lin[1]*

[1]*College of Pharmacy, Changchun University of Chinese Medicine, Changchun, 130117, China*
[2]*National Engineering Laboratory for Druggable Gene and ProteinScreening, Northeast Normal University, Changchun 130117, China*
[3]*Jilin Ginseng Academy, Changchun University of Chinese Medicine, Changchun, 130117, China*

Article Information
Received 02 July 2022
Revised 25 July 2022
Accepted 05 August 2022
Available online 29 March 2023 (early access)
Published 20 December 2023

Authors' Contribution
TW and XH conceived the research idea and designed the study. JH and GL visited the dairy farms and collected the data. ZL performed data analysis. TW wrote the manuscript.

Key words
Saposhnikoviae radix, Network pharmacology, Molecular docking, Antipyretic, Apoptosis

ABSTRACT

The aim of this study was to explore the antipyretic role and mechanism of Saposhnikoviae Radix (SR). To achieve the objectives TCM-ingredient-target network and PPI network were constructed by TCMSP, TTD, DisGenet, OMIM databases and Cytoscape 3.7.2 software, and topology analysis was performed on the PPI network. KEGG signaling pathways were analyzed using DAVID database, and molecular docking verification was performed on the core targets after topology analysis. Subsequently, 24 rats were randomly divided into control group, model group, wild high-dose group and wild low-dose group, 6 rats in each group. Results of *in vivo* experiments showed that high-dose group ($P<0.01$) and low-dose group ($P<0.01$) significantly decreased body temperature in rats; high-dose group significantly decreased TNF-α, IL-1β and IL-6 levels ($P<0.01$), and low-dose group significantly decreased TNF-α and IL-6 levels ($P<0.01$); high-dose group significantly decreased BAX, caspase3, COX2 and TNF-α protein expression levels in hypothalamus ($P<0.01$ or $P<0.05$), and low-dose group significantly increased BCL2 protein expression levels ($P<0.01$). It was found that SR can significantly inhibit lipopolysaccharide-induced fever in rats with elevated body temperature, reduce serum TNF-α, IL-1β and IL-6 levels, reduce the hypothalamus COX2, caspase3 and Bax protein expression levels and improve BCL2 protein expression levels, play an antipyretic effect.

INTRODUCTION

Fever is commonly found among clinical patients. It is generally caused by Pyrogen, which leads to the production of pyrogenic cytokines in the body under stress and thus accelerate the synthesis and release of prostaglandin E2 and cyclic adenylate in hypothalamus into the blood (Li and Li, 2020; Chen *et al*., 2022). Although fever is a specific manifestation of the body's defense function, it can also cause obvious discomfort to patients. According to traditional Chinese medicine, exogenous fever is a disease with fever as its main clinical manifestation caused by external pathogens such as wind, cold, summer heat, dampness, dryness and heat invading the body, including respiratory tract infections caused by bacteria and viruses (Cai *et al*., 2022). There have been several respiratory tract infectious diseases caused by viral infections in China, including H1N1, H5N1, H7N9, SARS and the recent outbreak of COVID-19, which have a wide spread, a large number of infected people and are characterized by fever (Jing-Chun *et al*., 2020; Jamieson and Rasmussen, 2021).

In recent years, Chinese medicine has made rapid progress in treating exogenous fever. Especially for exogenous fever caused by new pathogens, it is difficult for modern medicine to make judgment and drug intervention in a short time because of its rapid onset, rapid spread and serious condition. However, traditional Chinese medicine can effectively block the spread and deterioration of the disease through syndrome differentiation and treatment, which was fully reflected in the treatment of COVID-19 (Zhang *et al*., 2022; Huang *et al*., 2021). Doctors in the

* Corresponding author: linzhe_1966@163.com
0030-9923/2024/0001-0385 $ 9.00/0

past dynasties had applied traditional Chinese medicine prescriptions to treat exogenous fever, such as Fangfeng Tongsheng Pill and Xijiao Shengma Decoction. The Chinese patent medicines such as Jingfang Granule, and the substituted tea for prevention of COVID-19 introduced by various Chinese medicine hospitals, such as Yupingfeng Powder, were widely used in the initial treatment of COVID-19. Many of the above prescriptions contain Saposhnikoviae Radix (SR), which shows that SR plays an irreplaceable role in the prescription.

SR, as the dry root of Saposhnikovia divaricate (Turcz.) Schischk, is pungent, slightly sweet and warm in nature, and belongs to the liver, bladder and spleen channels. It has the functions of expelling wind, relieving exterior syndrome, eliminating dampness, relieving pain and spasmolysis (National Pharmacopoeia Commission, 2020). Traditional Chinese medicine (TCM) has a long history of applying SR. SR listed as the top grade in Sheng Nong's Herbal Classic, and used for common cold, headache, rheumatic arthralgia, rubella itching, tetanus and other diseases (Li *et al*., 2022; Shi *et al*., 2021). In recent years, a large number of pharmacological studies have shown that polysaccharide, volatile oil and coumarin in SR have antipyretic, anti-inflammatory and analgesic activities (Bai *et al*., 2020). Although SR has a potential therapeutic effect on fever, the specific mechanism of its antipyretic effect is not clear. Taking SR as the research object, this study applied the research method of network pharmacology to construct a SR-heating network, verified it by molecular docking technology and whole animal experiment, and explored the potential mechanism of SR's antipyretic effect, with the aim of providing theoretical basis for clinical application of the prescription preparation of SR.

MATERIALS AND METHODS

Animal experiment

Thirty five SPF healthy male SD rats aged 6-8 weeks, weighing 160-180 g, were provided by Changchun Yisi Experimental Animal Technology Co., Ltd., with the animal certificate number of SCXK- (J) -2020-0002. The rats were kept in the laboratory animal room of Changchun University of Traditional Chinese Medicine. During the feeding period, the rats drank and ate freely. The experimental process was reviewed by the ethics committee of Changchun University of Traditional Chinese Medicine, which met the welfare and ethical standards of experimental animals. The ethics number was 2021247.

Experimental reagents and instruments

Lipopolysaccharide (Beijing Solebao Technology Co., Ltd., batch number: L8880), wild SR (provided by Baishan Vocational and Technical College, identified by Chinese Medicine Resources Teaching and Research Section of Changchun University of Traditional Chinese Medicine, batch number: 2020901), pentobarbital sodium (Guangzhou Chemical Reagent Factory, batch number: 850601), IL-1β, IL-6, TNF-α(ELISA MM-0190R1, MM-0180R1), COX2 antibody, caspase3 antibody, Bax antibody, BCL2 antibody, secondary antibody (Wuhan PROTEINTECH Biotechnology Co., Ltd., article number: 12375-1-AP, 66470-2-lg, 50599-2-lg, 26593-1) Article number: WL01581), RIPA lysate, BCA protein concentration determination kit (Shanghai Beyotime Biotechnology Co., Ltd., article number: P0013B, P0010), protease inhibitor mixture (Shanghai Yami Biomedical Technology Co., Ltd., article number: GRF101), PMSF (Wuhan Service Biotechnology Co., Ltd., article number: G2008), Freeze centrifuge (Hunan Xiangyi Laboratory Instrument Development Co., Ltd., model: TGL-16), Invitrogen iBright imaging system (Thermo Company, USA, model: CL750), PowerPac™basic electrophoresis apparatus (Bio-Rad Company, USA, model: 1645050).

Screening of SR active ingredients and target prediction

TCMSP database was used to collect the information of chemical ingredients of SR (Ru *et al*., 2014), and the active ingredients on the condition of oral bioavailability (OB) ≥ 30% and drug-like property (DL) ≥ 0.18 were screened (Li *et al*., 2015).

Prediction of active compound targets

The collected active ingredients were input into PubChem database to query its SMILE number, and then input into Swiss target prediction platform, and their 2D structure was used to predict the target. The target name was standardized to the official gene symbol by using UniProKBt search function in UniProT database.

Construction of TCM-ingredient-target network

After mapping the finished windbreak active ingredients and corresponding targets, the node file and attribute file were established and then imported into Cytoscape 3.7.2 software with the parameters of each node adjusted for visualization. In this way, "TCM-ingredient-target" network of SR was constructed.

Disease target prediction

TTD database, DisGenet database, OMIM database, CTD database and PharmaGKB database were used to search for the corresponding targets of fever, and the keyword "FEVER" was used to search for the targets. After sorting, UniProKBt was used for standardization.

Common target screening and protein-protein interaction network analysis

Bioinformatics and evolutionary genomics platform (http://bioinformatics.psb.ugent.be/webtools/Venn/) was used to screen and visualize common targets of SR-fever, SR-inflammation and SR-fever-inflammation. The common targets were imported into String (https://string-db.org/) platform, species were selected as "*Homo sapiens*", and other parameters were used as default to construct the protein interaction network. The TSV files obtained were imported into Cytoscape 3.7.2 software, and topology analysis was conducted on the condition that degree was greater than 2 times of its median. Moreover, MODE plug-in was used for cluster analysis, and the network with the highest MODE score was selected for visualization.

Molecular docking

The cluster results of common targets of SR-fever obtained in 1.6 were used as the core targets of SR to exert antipyretic and anti-inflammatory effects. The 3D structure of the core target protein was searched and downloaded using RCSB PDB database, and the 3D structure of the protein was extracted by using Pymol 2.4.0 software for water removal. The 3D structure of the active ingredients corresponding to the core targets was searched by Pubchem database and then downloaded. Using Autodock Tools1.5.6 software, the active ingredients corresponding to the core targets were semi-flexibly docked with the targets, and the results with the binding energy less than -5.0 KJ/mol were input into Discovery Studio 2020 for visualization.

GO analysis and KEGG pathway analysis

DAVID 6.8 platform (https://david.ncifcrf.gov/) and R software were used to analyzed the KEGG pathways of common targets of SR-fever. The species was selected as "homo sapiens", the target type was "gene List", and the symbol was "OFFICIAL GENE SYMBOL". After submission, KEGG pathway analysis was performed, and the KEGG pathway analysis results were imported into R software for visualization.

Preparation of decoction of SR

Wild products of SR were dried in the shade, and cut into pieces weighted 500 g. The pieces were soaked in water for 30 min in a ceramic decoction pot, then decocted for 30 min, and finally concentrated to 1 $g \cdot mL^{-1}$. The dosage of low-dose wild SR group was 0.45 $g\ kg^{-1}$, and that of high-dose wild SR group was 0.90 $g\ kg^{-1}$.

Experimental animal modeling and drug administration

Before modeling, the rectal temperature of male rats was measured twice a day, and the rats with abnormal body temperature and large body temperature change (> 0.3°C) were excluded. The rest rats we are randomly divided into blank group (n=6), model group (n=6), low-dose wild Saposhnikovia divaricata group (YD, n=6) and high-dose wild Saposhnikovia divaricata group (YG, n=6). After 3d of adaptive feeding, except the blank group, the rest groups were injected with LPS ($100\mu g \cdot kg^{-1}$) intraperitoneally, and the drug solution ($10mL \cdot kg^{-1}$) was given by gavage 30 min after modeling, while the blank group was injected with the same amount of normal saline. Water was fasted before modeling, and administration was performed 30min after modeling.

Body temperature measurement of rats

A day before the experiment, the hair on the back and neck of rats was shaved with a barber scissors to expose the skin. The infrared forehead thermometer was attached to the exposed skin to detect the body temperature. The average temperature was measured 3 times before modeling, and recorded every 1h after modeling. The electronic thermometer measured the temperature 3 times and recorded the average value. The temperature curves of each group were drawn after continuous monitoring for 8h.

Detection of the levels of TNF-α, IL-1β and IL-6

After the experiment, pentobarbital sodium ($40mg\ kg^{-1}$) was injected into the abdominal cavity to anesthetize the rats. After that, the blood was collected from abdominal aorta, and centrifuged at 3500r/pm for 10min to separate the serum and store them at -20°C for later use. After thawing the serum, the kit was balanced at room temperature for 30min. The standard, antibody, enzyme and working fluid required for the experiment were prepared in advance. The serum absorbance of the sample was measured at 450nm under a microplate tester according to the operating procedures prescribed in kit, based on which, the expression levels of TNF-α, IL-1β and IL-6 in serum were finally obtained.

Detection of the expression levels of COX2, TNF-α, caspase3, Bax and Bcl2 proteins in hypothalamus of rats

After blood collection, the whole brain of rat was taken out quickly. The hypothalamus was taken between the optic chiasma and the gray tubercle, placed in EP tube and stored in liquid nitrogen. The expressions of COX2, TNF-α, caspase3-3, Bax and Bcl2-2 proteins in hypothalamus of rats in each group were detected by Western blotting. Rat hypothalamus (40 mg) was homogenized and lysed in RIPA lysis buffer, and centrifuged at 12000 rpm^{-1} (4°C) for 10min. Supernatant was collected, and protein concentration was detected with BCA protein detection kit. The supernatant was stored at -80°C for later use. SDSPAGE

gel was prepared. After electrophoresis, the membrane was transferred to PVDF, sealed, and primary and secondary antibodies were incubated. ECL chemiluminescence method was used for exposure and development in the imaging system, and then Image J software was used for quantitative analysis of optical density.

Statistical methods

SPSS 21.0 software was used for statistical analysis. The expression levels of body temperature, TNF-α, IL-1β and IL-6 in serum and COX2, TNF-α, caspase3, Bax and Bcl2 protein in brain tissues of rats in each group were all in accordance with normal distribution, which was expressed as $x \pm s$. One-way ANOVA was used for comparison of sample averages among groups, and LSD-t test was used for pairwise comparison among groups. $P < 0.05$ indicated statistically significant difference.

RESULTS

Ingredient screening and target prediction

A total of 18 active ingredients including isoimperatorin, wogonin and sitosterol in SR were screened through TCMSP database. Some active ingredients are shown in Table I. The predicted target number of active ingredients is 545. The TCM-ingredient-target relationship was visualized by Cytoscape 3.7.2 software, and the top 5 active ingredients in degree were selected as the core ingredients for visualization. The network of TCM-ingredient-target was constructed as shown in Figure 1.

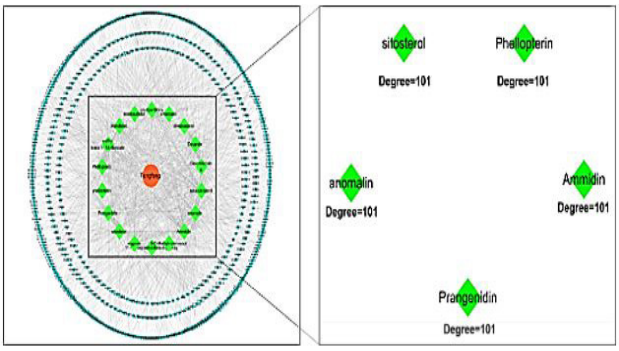

Fig. 1. TCM-ingredient-target network diagram.

Table I. Screening results active ingredients of SR.

Molecule ID	Molecule name	OB (%)	DL	2D structure	PubChem CID
MOL000011	Cleomiscosin A	68.83	0.66	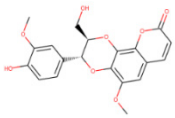	442510
MOL011732	Anomalin	59.65	0.66	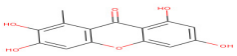	6859585
MOL001941	Ammidin	34.55	0.22	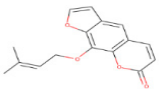	10212
MOL011747	Ledebouriellol	32.05	0.51	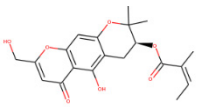	NA
MOL011753	5-O-Methylvisamminol	37.99	0.25	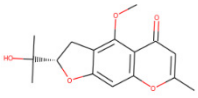	441970
MOL002644	Phellopterin	40.19	0.28	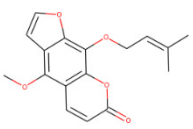	98608

Disease target prediction and common target analysis

Through TTD database, DisGenet database, OMIM database, CTD database and Pharm GKB database, 1189 fever targets were obtained. There are 135 targets for screening windproof and fever, and the Venn diagram is shown in Figure 2. The common targets were uploaded to the String platform for protein-protein interaction analysis, and the analysis results were imported into the network. The software Cytoscape 3.7.2 was used for topology analysis. For the SR-Fever network, the genes with top 5 degree values were selected as the core genes, including caspase3, MAPK8, PIK3CA, BCL2 and ESR1. The results are shown in Figure 3.

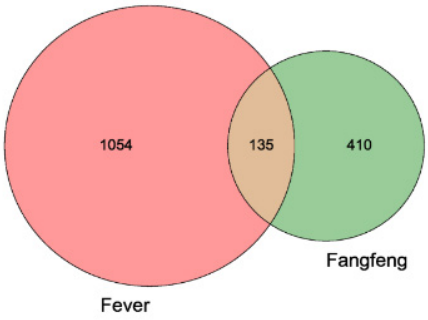

Fig. 2. The intersection of SR-Fever targets.

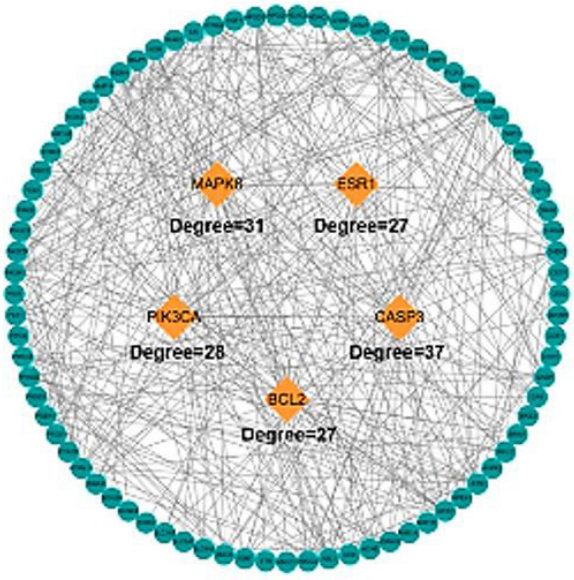

Fig. 3. PPI network of SR-fever targets.

GO analysis and KEGG pathway analysis

To further explore the antipyretic mechanism of SR, KEGG pathway analysis was made on the common target of SR-fever in 2.2. The enriched results were sorted according to P value, as shown in Figure 4. The antipyretic effect of SR involves neurotrophic signal pathway, apoptosis, epidermal growth factor receptor signal pathway and fork-like transcription factor signal pathway, among which apoptosis regulation pathway was highly enriched.

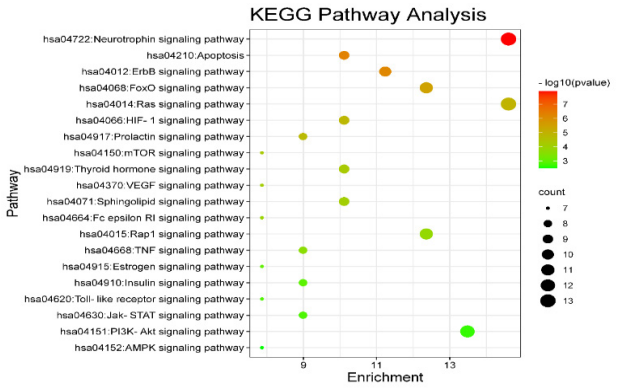

Fig. 4. Analysis of the KEGG pathway of antipyretic effect of SR.

Molecular docking analysis

The protein crystal structures of the five core targets caspase 3, MAPK8, PIK3CA, BCL2 and ESR1 obtained in 2.2 were input into Antodock Tool 1.5.6 software for hydrogenation and charge calculation, and then docked with the corresponding core ingredients, respectively. The docking results are shown in Table II and Fig. 5. Under the condition that the binding energy is less than -5.0 KJ/mol, most ingredients have strong binding activity with the target.

Table II. Docking results of core targets and active ingredients.

Core targets	Corresponding ingredients	Binding energy (-kJ/mol)
ESR1	Sitosterol	-6.77
BCL2	Anomalin	-6.03
Caspase3	Prangenidin	-5.41
PIK3CA	Phellopterin	-5.32
MAPK8	Ammidin	-5.03

Body temperature of rats

After subcutaneous injection of LPS, the body temperature of rats in each group increased. Compared with the blank group, the body temperature of rats in the model group increased significantly at 2h, 3h, 4h, 5h,6h, 7h and 8h after LPS injection ($P < 0.05$ or $P < 0.01$).

Table III. The body temperature of rats (n=6, $\bar{x} \pm s$).

	Temperature (°C)							
Group	**1h**	**2h**	**3h**	**4h**	**5h**	**6h**	**7h**	**8h**
CT	36.8±0.3	37.3±0.3	37.9±0.7	37.9±0.1	37.5±0.3	37.7±0.1	37.3±0.6	37.6±0.3
M	37.3±0.2	38.7±0.4##	39.3±0.3#	39.9±0.3##	39.8±0.3##	39.3±0.2##	39.3±0.0##	39.2±0.2##
YG	37.1±0.4	38.1±0.5	37.7±0.3**	38.4±0.1**	38.6±0.2**	38.5±0.5**	37.6±0.1**	38.1±0.2**
YD	36.9±0.5	38.0±0.5	38.7±1.2	39.5±0.8	39.1±0.7*	39.2±0.5	39.4±0.4	39.1±0.3

##P<0.01, #P<0.05 *vs* control group; **P<0.01, *P<0.05 *vs* model group. CT, blank group; M, model group; YG, high-dose wild SR; YD, low-dose wild SR.

Compared with the model group, the body temperature of rats in high-dose wild SR group decreased significantly at 3h, 4h, 5h, 6h, 7h and 8h after LPS injection (P < 0.01), while that of rats in low-dose wild SR group decreased significantly at 5h after LPS injection (P < 0.01). The results are shown in Table III.

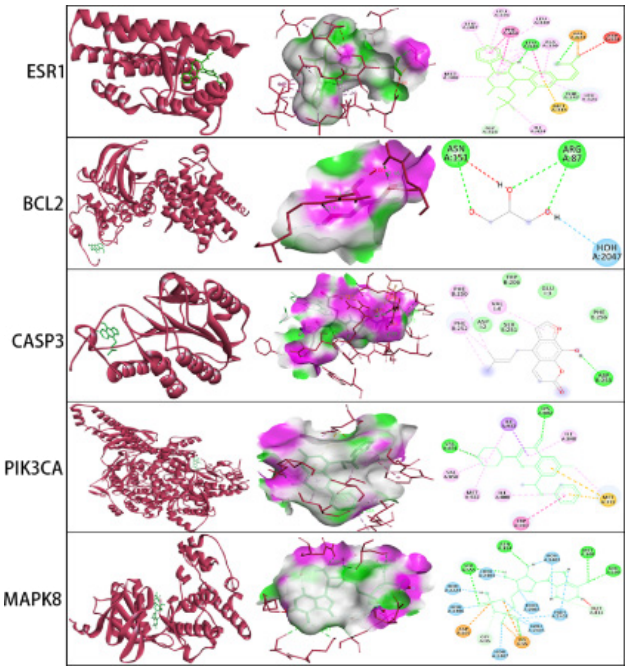

Fig. 5. Molecular docking visualization results.
Note: From left to right, the above figure is the 3D overall figure of molecular docking, hydrogen bond interaction figure and 2D interaction diagram; in the figure on the left side, red is the target protein structure, and green is the molecular structure of the ingredient; in the figure at the middle position, green is the hydrogen bond donor, and purple is the hydrogen bond acceptor.

Levels of serum TNF-α, IL-1β and IL-6 in rats

Compared with the blank group, the levels of serums TNF-α, IL-1β and IL-6 in rats of the model group were significantly higher according to ELISA detection (P < 0.01). Compared with the model group, the levels of serums TNF-α, IL-1β and IL-6 in rats of the high-dose wild SR group significantly decreased (P < 0.01), and those in rats of the low-dose wild SR group significantly decreased (P < 0.01). The results are shown in Table IV.

Table IV. The levels of serums TNF-α, IL-1β and IL-6 in rats.

Group	TNF-α (ng/L)	IL-1β (ng/L)	IL6 (pg/mL)
CT	50.85±0.71	13.73±3.69	17.70±1.37
M	102.15±1.76##	24.88±4.29##	37.96±1.05##
YG	70.97±7.94**	14.79±0.97**	23.89±1.59**
YD	74.01±6.82**	19.67±1.90**	28.78±3.21

##P<0.01 *vs* control group; **P<0.01 *vs* model group. For details of groups, please refer to Table III.

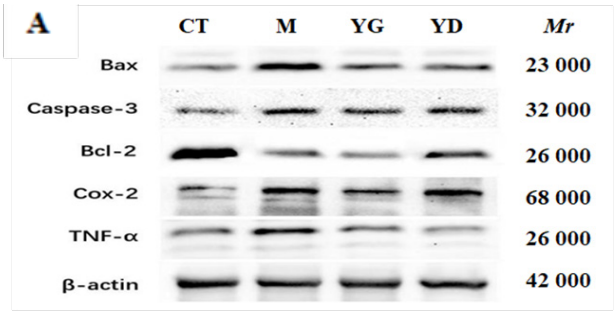

Fig. 6. The expression levels of COX2, TNF-α, BAX, caspase3 and BCL2 proteins in the hypothalamus of rats in each group. For details of groups, please refer to Table III.

Expression levels of COX2, TNF-α and apoptosis pathway protein in hypothalamus of rats

Western blotting showed that compared with the blank group, the expression levels of BAX and caspase 3 in hypothalamus of rats in the model group significantly increased (P < 0.01) and decreased (P < 0.01). Compared with the model group, the expression levels of BAX and caspase 3 in hypothalamus of rats in the SR decoction group significantly decreased (P < 0.05 or P < 0.01), and

those of rats in the low-dose wild SR group significantly decreased; compared with the blank group, the expression level of COX2 protein in hypothalamus of rats in the model group significantly increased ($P < 0.01$), while that of rats in the high-dose wild SR group significantly decreased ($P < 0.01$). Compared with the blank group, the expression level of TNF-α protein in the hypothalamus of rats in the model group significantly increased ($P < 0.01$), while that of rats in the high-dose wild SR group significantly decreased ($P < 0.01$). See Figure 6 for the results.

DISCUSSION

Modern research has proved that the agglutination of pyrogen factors and the participation of innate immune response are the central links to kill pathogens and lower body temperature (Song *et al*., 2017). In addition to the regulated rise of body temperature, fever can also cause various diseases, changes in metabolism and physiological characteristics of the body system, and changes in immune response (Dai *et al*., 2021; Zheng *et al*., 2021). The TCM theories hold that fever is caused by exogenous pathogenic factors, which suppress the muscle surface. The yang qi can't reach outside, and the healthy qi competes with the pathogenic qi, then causing fever (Zhang and Xie, 2016). Although ancient and modern doctors have used SR to treat widespread exogenous fever, the specific molecular mechanism of SR and antipyretic is still unclear. Therefore, this study systematically explored the material basis and potential molecular mechanism of SR to treat exogenous fever by using network pharmacology and molecular docking technology. The results showed that the core active ingredients of SR with antipyretic effect were Sitosterol, Phellopterin, Prangenidin, Ammidin and Anomalin. In addition, PPI protein interaction analysis and KEGG pathway analysis showed that there was a significant accumulation in the apoptosis pathway of SR, so it was speculated that the mechanism of SR antipyretic action may focus on regulating core targets such as ESR1, caspase3, BCL2, PIK3CA and MAPK8.

COX-2 is the key enzyme for synthesizing prostaglandin E2, which plays an important role in the process of fever as the key intermediate of body temperature rise. Some studies have shown that after subcutaneous injection of dry yeast causes fever in rats, activating p65 protein into nucleus promotes the up-regulation of COX-2 gene expression in hypothalamus (Cheng *et al*., 2022). TNF-α, IL-1β and IL-6, as the main cytokines, are involved in the occurrence of acute inflammation. They can increase the adhesion between monocytes and macrophages, vascular endothelial cells and neutrophils, induce cells to release free radicals and hydrogen peroxide, and enhance their ability to kill microorganisms (Jia *et al*., 2022). When the body temperature is abnormally elevated, the levels of TNF-α, IL-1β and IL-6 in serum show an obvious upward trend (Zhou *et al*., 2018; Ye *et al*., 2020). In this study, animal experiments have proved that wild SR can significantly reduce the expression level of COX2 protein in hypothalamus, and inhibit the increase of body temperature induced by LPS in rats, and reduce the levels of TNF-α, IL-1β and IL-6 in serum. All these significantly reduce the inflammatory reaction of the body and lower the body temperature.

In addition, some studies have found that inflammatory factors such as IL-6, IL-1β, TNF-α can act on the hypothalamus of the thermoregulation center by acting on the receptor release signals expressed in the blood-brain barrier cerebrovascular system, which will raise the temperature set point and eventually lead to fever (Schiltz and Sawchenko, 2002). Under normal physiological conditions, the blood-brain barrier can isolate the brain from inflammatory factors in the blood, and prevent the brain from being exposed to the stimulation of inflammatory factors. Some studies have suggested that excessive body temperature and the stimulation of inflammatory factors can cause the apoptosis of blood-brain barrier cells and damage the blood-brain barrier (Li and Liu, 2004; Zhou *et al*., 2018). Because of the damage of blood-brain barrier, more inflammatory factors enter the brain and continue to stimulate the hypothalamus, further causing the temperature set point to rise, thus causing the body to have high fever. Therefore, our research group speculated that reducing the apoptosis of hypothalamic tissue cells and maintaining the integrity of hypothalamic blood-brain barrier would help to restore the body's thermoregulation. When cells are stimulated by external or internal channels, Bcl2-2 protein is inhibited, but Bax protein of the same family is highly expressed, and then signal cascade is activated to recruit caspase family proteins to cut various cell macromolecules, which leads to cell apoptosis (Hu *et al*., 2021; Li *et al*., 2020; Liu *et al*., 2020), among which caspase-3 is a typical one. The external pathway of cell apoptosis is mediated by death-inducing ligands, such as Fas ligand, TNF-α and TRAIL, which bind to death receptors, thus transmitting apoptosis signals (Lin *et al*., 2022; Zhang *et al*., 2020). Vivo experiments in this study found that the expression levels of TNF-α protein. In hypothalamus of rats in the model group increased, which indicated that LPS might activate the external apoptosis pathway. The expression of TNF-α protein was down-regulated in all dose groups of wild SR, which indicated that Fangfeng Decoction could inhibit TNF-α-mediated apoptosis in hypothalamus. At the same time, the experimental results showed that wild

SR could significantly up-regulate the expression level of Bcl2-2 protein in rat hypothalamus, and down-regulate the expression level of Bax and caspase3-3 protein, indicating that it could alleviate the hypothalamic tissue damage of LPS-induced fever model rats by inhibiting the process of apoptosis and play an antipyretic role. Fever is considered an internal infection. In fact, in the heat of a fever, many germs are unable to grow. Of course, there is much debate about the uselessness of fever.

CONCLUSION

In this study, molecular docking and in vivo experiments showed that the active ingredients in SR had strong binding activity with ESR1, PIK3CA and MAPK8. This indicated that SR probably activated the upstream ESR1, PIK3CA and MAPK8 sites, inhibited the apoptosis of hypothalamus tissue, reduced hypothalamus injury, maintained the integrity of blood-brain barrier in hypothalamus, prevented inflammatory factors from entering hypothalamus, reduced the stimulation of inflammatory factors to hypothalamus thermoregulation center, restored body thermoregulation function and played an antipyretic role.

ACKNOWLEDGEMENTS

The research is supported by (i) Administration of Traditional Chinese Medicine of Jilin Province, Effect of toad oil on intestinal microbial diversity and antidepressant effect in depression model mice (NO., 2022014); (ii) Department of Science and Technology Jilin Province, Study on the secondary development of guiling tablets, (NP., 20210401067YY).

Statement of conflict of interest

The authors have declared no conflict of interest.

REFERENCES

Bai, G., Wang, C., Li, J., Li, L., and Yao, J., 2020. Research progress of active ingredients and physiological effects of Chinese herbal medicines against wind. *China's Naturopathy*, **28**: 116-117.

Cai, X., Ma, X., Liu, N., and Xu, L., 2022. Research progress of treating fever with traditional Chinese medicine. *Guangming J. Chinese Med*., **37**: 1093-1096.

Chen, S., Li, X., Wang, W., Du, W., and Li, M., 2022. Research progress on antipyretic effect of Chinese medicine. *Chinese J. clin. Pharmacol. Ther*., **27**: 334.

Cheng, Y., Xu, J., Zeng, R., Zhao, X., Gao, W., Quan, J., Hu, X., Shen, Z., and Zhang, J., 2022. The role of prostaglandin E2 synthesized in rat lateral parabrachial nucleus in LPS-induced fever. *Neuroendocrinology,* **112**: 399-416. https://doi.org/10.1159/000518491

Dai, L., Dai, L., Dai, C., Chen, Y., and Liu, Z., 2021. Study on antipyretic effect of indigo naturalis on endogenous pyrogenic fever rabbits and its mechanism. *Strait Pharm. J*., **33**: 13-16.

Hu, S., Wang, Y., Xu, Z., and Zhou, J., 2021. Research progress of the role of Bcl-2 family molecules in apoptosis. *Prog. Vet. Med*., **42**: 85-89.

Huang, K., Zhang, P., Zhang, Z., Youn, J., Zhang, H., and Cai, H., 2021. Traditional Chinese Medicine (TCM) in the treatment of COVID-19 and other viral infections: Efficacies and mechanisms. *Pharmacol. Ther*., **225**: 107843. https://doi.org/10.1016/j.pharmthera.2021.107843

Jamieson, D.J., and Rasmussen, S.A., 2021. An update on COVID-19 and pregnancy. *Am. J. Obstet. Gynecol*.,

Jia, R., Li, C., Li, S., Yang, J., and Dai, X., 2022. Effects of herba ephedrae and ramulus cinnamomi on IL-6, IL-1β and TNF-α in lung tissue of rats with fever. *World J. Integr. Trad. Western Med*., **17**: 22-26, 37.

Jing-Chun, S., Gang, W., Zhang, W., Zhang, Y., Wei-Qin, L.I. and Zhou, Z., 2020. Expert consensus for diagnosis and treatment of coagulation dysfunction in COVID-19. *Med. J. Chinese People's Liberation Army*, **45**: 335-344.

Li, C., and Li, Y., 2020. Analysis on the medication rule of Chinese patent medicine for fever based on the auxiliary platform of traditional Chinese medicine inheritance. *Mod. J. Integ. Trad. Chinese Western Med*., **29**: 381-385.

Li, J., Zhao, P., Li, Y., Tian, Y. and Wang, Y., 2015. Systems pharmacology-based dissection of mechanisms of Chinese medicinal formula Bufei Yishen as an effective treatment for chronic obstructive pulmonary disease. *Sci. Rep*., **5**: 1-15. https://doi.org/10.1038/srep15290

Li, X., Li, H., Wang, T., Zhao, Y., and Shao, Y., 2022. Network pharmacology-based analysis of the mechanism of Saposhnikovia divaricata for the treatment of type I allergy. *Pharm. Biol*., **60**: 1224-1236. https://doi.org/10.1080/13880209.2022.2086583

Li, Y., and Liu, Y., 2004. Brain injury and fever. Foreign medicine. *J. Int. Neurol. Neurosurg*., **6**: 585-588.

Li, Y., Zhang, Z., Zhao, Y., Yi, J., and Wang, Q., 2020. Research progress of Bcl-2 family on apoptosis

and autophagy of hepatocellular carcinoma. *J. Mudanjiang Med. Coll*., **41**: 141-144.

Lin, S., Qian, H., Lu, J., and Xiao, M., 2022. Research progress of caspase family involved in the absorption of apoptosis in dental pulp tissue by deciduous teeth root. *Stomatology*, **42**: 180-183.

Liu, D., Li, B., and Li, H., 2020. Research progress of caspase family, the core gene of apoptosis. *Chinese J. Med. Guide*, **22**: 800-805.

National Pharmacopoeia Commission, 2020. *Pharmacopoeia of the People's Republic of China (2020 edition 1)*. Medical Science and Technology Press, Beijing, China. 2020: 156.

Ru, J., Li, P., Wang, J., Zhou, W., Li, B., Huang, C., Li, P., Guo, Z., Tao, W., Yang, Y., and Xu, X., 2014. TCMSP: A database of systems pharmacology for drug discovery from herbal medicines. *J. Cheminf*., **6**: 1-6. https://doi.org/10.1186/1758-2946-6-13

Schiltz, J.C., and Sawchenko, P.E., 2002. Distinct brain vascular cell types manifest inducible cyclooxygenase expression as a function of the strength and nature of immune insults. *J. Neurosci.,* **22**: 5606-5618. https://doi.org/10.1523/JNEUROSCI.22-13-05606.2002

Shi, L., Meng, X., Cao, S., Sun, J., and Pei, L., 2021. Herbal traceability of Saposhnikoviae Radix. *Res. Pract. Chinese Med*., **35**: 93-97.

Song, Y., Ren, Y., Ji, H., and Gong, X., 2017. Research progress of molecular mechanism of fever. *J. Pharm. Res*., **36**: 99-103.

Ye, H.B., Zuo, J.H., Ma, C., Lin, H., Xu, Y., Sun, J.M., Ye, D.D., Lv, G.F. and Lin, Z., 2020. Study on the antipyretic effect of gypsum and its compatibility on yeast-induced pyrexia rats based on NF-κB signaling pathway. *Mater. Exp*., **10**: 748-755. https://doi.org/10.1166/mex.2020.1691

Zhang, B., and Xie, F., 2016. Discuss the relationship between fever and sweating from the theory of traditional Chinese medicine. *Shaanxi J. Trad. Chinese Med*., **37**: 1644-1645.

Zhang, J., Shao, L., Tong, T., Liu, L., and Ying, R., 2020. Research progress of NF-κB and neutrophil apoptosis. *J. Med. Theory Pract*., **33**: 886-888.

Zhang, S., Yang, Z., Chen, Z.L., Li, Z.N., and Yue, S.J., 2022. Efficacy and safety of three Chinese patent medicines and three TCM prescriptions for COVID-19: A systematic review and network meta-analysis. *Evid. Based Complement. Altern. Med*., **2022**. https://doi.org/10.1155/2022/4654793

Zheng, N., Li, X. and Wu, Y., 2021. Effect of yinqiao baihu decoction combined with ibuprofen on symptoms and inflammatory response of children with exogenous fever. *Mod. Med. Hlth. Res. Electron. J*., **5**: 135-138.

Zhou, B., Chen, Y., Feng, L., Wang, Z., and Wu, L., 2018. Effect of gypsum japonica rice soup on antipyretic and anti-inflammatory effects and expression of nuclear factor -κBp65 and cyclooxygenase -2 in rats with fever caused by dry yeast. *Sci. Technol. Eng*., **18**: 165-170.

Zhou, X.Y., Yu, M., and Cui, H.X., 2018. Correlation of the changes of blood brain barrier permeability with the activation of apoptosis, inflammatory response and stress response in rats with cerebral hemorrhage. *J. Hainan Med. Univ. (Eng. Ver.)*, **24**: 1-4.